

PROCEEDINGS OF SPIE

[SPIDigitalLibrary.org/conference-proceedings-of-spie](https://spiedigitallibrary.org/conference-proceedings-of-spie)

TuMore: generation of synthetic brain tumor MRI data for deep learning based segmentation approaches

Lydia Lindner, Birgit Pfarrkirchner, Christina Gsaxner, Dieter Schmalsteig, Jan Egger

Lydia Lindner, Birgit Pfarrkirchner, Christina Gsaxner, Dieter Schmalsteig, Jan Egger, "TuMore: generation of synthetic brain tumor MRI data for deep learning based segmentation approaches," Proc. SPIE 10579, Medical Imaging 2018: Imaging Informatics for Healthcare, Research, and Applications, 105791C (6 March 2018); doi: 10.1117/12.2315704

SPIE.

Event: SPIE Medical Imaging, 2018, Houston, Texas, United States

TuMore: Generation of Synthetic Brain Tumor MRI Data for Deep Learning Based Segmentation Approaches

Lydia Lindner^{a,b}, Birgit Pfarrkirchner^{a,b}, Christina Gsaxner^{a,b}, Dieter Schmalstieg^a and Jan Egger^{a,b,c}

^a TU Graz, Institute for Computer Graphics and Vision, Inffeldgasse 16c/II, 8010 Graz, Austria

^b Computer Algorithms for Medicine (Cafe) Laboratory, 8010 Graz, Styria, Austria

^c BioTechMed-Graz, Krenngasse 37/1, 8010 Graz, Austria

ABSTRACT

Accurate segmentation and measurement of brain tumors plays an important role in clinical practice and research, as it is critical for treatment planning and monitoring of tumor growth. However, brain tumor segmentation is one of the most challenging tasks in medical image analysis. Since manual segmentations are subjective, time consuming and neither accurate nor reliable, there exists a need for objective, robust and fast automated segmentation methods that provide competitive performance. Therefore, deep learning based approaches are gaining interest in the field of medical image segmentation. When the training data set is large enough, deep learning approaches can be extremely effective, but in domains like medicine, only limited data is available in the majority of cases. Due to this reason, we propose a method that allows to create a large dataset of brain MRI (Magnetic Resonance Imaging) images containing synthetic brain tumors - glioblastomas more specifically - and the corresponding ground truth, that can be subsequently used to train deep neural networks.

Keywords: Synthetic Brain Tumor, Glioblastoma, Segmentation, Deep Learning, Data Augmentation, hybrid MRI.

1. DESCRIPTION OF PURPOSE

In current clinical practice, the interpretation of medical images is mainly done by human experts such as radiologists and physicians [1]-[7]. MRI (Magnetic Resonance Imaging) images are assessed either based on qualitative criteria, for example characteristic hyper-intense tissue occurrence in contrast-enhanced T1-weighted MRI images, or by relying on basic quantitative measures as the largest axial diameter of the tumor [8]. Since manual segmentation of brain tumors is time consuming, subjective and prone to error, there exists a need for fast, objective and precise automated segmentation methods. Therefore, deep learning based approaches gain increasing interest in the field of medical image segmentation.

When the training data set is large enough, deep learning approaches can be extremely effective. However, in the medical field there are usually only limited data samples available, since medical data is heavily protected due to privacy concerns. Hence, one big challenge of using deep learning approaches for medical image segmentation lies in augmenting the available data set to build deep models without overfitting the training data. A basic common and accepted technique for augmenting image data is to perform geometric and color augmentations [1], [9]. Instead of using these basic data augmentation techniques, our approach generates synthetic glioblastomas and insert them into MRI scans of healthy subjects. The resulting "hybrid" MRI images can subsequently be used to train a deep neural network for automatic tumor segmentation.

Glioblastomas (GBMs) are rather large tumors that have thick, irregular-enhancing margins with a central necrotic core [10], [11]. Since it is not possible for the brain to move outside the surrounding skull and thereby make room for a growing mass, tumors displace and compress the surrounding brain tissue. This process is called the tumor mass effect [12]. In clinical practice of oncology and diagnostic medicine, typically only the enhancing tumor and necrotic core are segmented, since these regions are of primary interest. Segmentations of structures other than brain tumor are usually not done, since the segmentation of edema etc. is extremely challenging and will therefore not represent truth very well [13]. Hence, with the proposed method, only the enhancing tumor and necrotic core of a glioblastoma are simulated as well as the tumor mass effect.

For the implementation of the proposed method, we used MeVisLab, a rapid prototyping and development platform for medical image processing, visualization, and image interaction. Image processing and interactive image manipulation can be achieved by building networks that are constructed of preexisting modules, macro modules created via Python scripting, and individual modules implemented in C++ [14]-[17].

2. METHODS

The tumor generation algorithm was based on a special type of polyhedron, namely an icosahedron. A regular icosahedron has 12 polyhedron vertices, 30 polyhedron edges and 20 equivalent equilateral polyhedron faces [18]. In order to receive an approximation of a sphere, the icosahedron was recursively refined, by dividing each of the existing faces into three equivalent equilateral triangles and repeating the procedure five times [19]-[21]. This results in a polyhedron with 2432 polyhedron vertices, which is called the “tumor base”. In order to obtain the typical irregular shape of a glioblastoma, a special displacement algorithm was applied to the vertices of the tumor base. The idea behind this displacement algorithm is to randomly choose one vertex (V_{chosen}) of the polyhedron, according to a uniform distribution. Then, the distance between V_{chosen} and the center of the polyhedron is increased. This results in an elevation of the corresponding vertex. To make the deformation look natural, also the remaining vertices are displaced accordingly. In order to determine the strength of displacement for each vertex - which decreases by distance to V_{chosen} - all vertices are categorized in displacement levels k , according to the minimum number of edges that are required to reach V_{chosen} (for example, direct neighbor vertices of V_{chosen} are in displacement level $k=1$). Finally, the displacement of V_{chosen} and the remaining vertices is achieved by multiplying the x , y and z coordinate of each vertex with factor $\varepsilon(k)$, that is defined by formula (1), where k denotes the displacement level of the corresponding vertex, d (which is randomly chosen according to a uniform distribution on the interval [1, 2.5]) indicates the initial strength of displacement and m is a decay factor of 0.97.

$$\varepsilon(k) = \begin{cases} 1 + d, & k = 0 \\ 1 + d \cdot m, & k = 1 \\ 1 + d \cdot m^{2k}, & k > 1 \end{cases} \quad (1)$$

This process of randomly choosing a vertex, displacing it and subsequently displacing the remaining vertices is repeated for altogether seven times. A simplified tumor mass effect was simulated by deforming the brain MRI image around the artificial glioblastoma according to a displacement field. For this purpose, the "ImageWarp" Module of MeVisLab - which performs backwards deformation – was applied. A simple sphere with variable radius was used to calculate the dense vector field. Since the force, that is applied to the brain by a tumor mass, is an outward radial force, that originates from the initial tumor region and weakens by distance [13], the required displacement field was constructed in the following way: First, the 3D Euclidean distance transform of the sphere was calculated to receive a gradually decreasing intensity from the tumor center to the edges. Then, a gradient filter was applied to the Euclidian distance transform, leading to a dense vector field. Afterwards, the Euclidian distance transform was normalized and multiplied with a factor, that can be varied depending on the desired strength of deformation. Finally, the result was multiplied with the previously calculated gradient field. This leads to a displacement field that lets the strength of the deformation weaken by distance. The network implemented in MeVisLab can be seen in Figure 1. An existing MRI image of a healthy subject is loaded into the framework and is subsequently reformatted to axial view. Additionally, the intensity range of the image is adjusted according to a reference. The *SetSeedPoint* module is used to manually set a seed point (by simply clicking on the desired position in the MRI scan) at which the artificial glioblastoma will be inserted. This is done to ensure that the tumor is located within the brain region. The individual *GenerateTumor* module is used to generate artificial glioblastomas by using the previously described algorithm. The synthetic tumor is provided at the output as visual scene graph (Inventor Scene) and has to be voxelized and further processed to comply with the basic radiographic features of real glioblastomas as they are visible in post-contrast T1-weighted (T1Gd) brain MRI scans. This is done with the *ProcessTumor* module. First, the tumor has to be translated according to the selected seed point. Then, a filled voxelization (fill color is a dark gray, which represents necrosis) is applied. Afterwards, a border is added to the tumor surface (color is a light gray, which represents the contrast enhanced surface). The voxelized tumor is slightly blurred to smooth the edges between the fill color and the edge color. Uniform noise is added to achieve a realistic looking appearance of the tumor. Furthermore, the *ProcessTumor* module is used to insert the synthetic glioblastoma into the existing MRI image and create the corresponding ground truth by using the *IntervalThreshld* module of MeVisLab. The internal network of this module can be seen in Figure 2. The *DeformationOfBrainMass* Module is used to simulate the tumor mass effect according to the previously described algorithm. In order to manually set a seed point (again by clicking on the desired position in the MRI scan) that defines the center of the brain mass deformation, the *SetSeedPointDeform* module can be used. The final brain MRI image (containing the synthetic glioblastoma) and the corresponding ground truth are saved as single slices in TIFF format using the *SaveSlices* module, which is an adapted version of the *SaveAsSingleSlices* module from related work [22]. The corresponding MeVisLab network and the C++ / Python source code is freely available [23]. MRI data used in this work was obtained from the Human Connectome Project (HCP) database [24]-[26]. *The 1200 Subjects Data Release* contains 3T MR imaging data from 1206 healthy young adult participants (1113 with structural MR scans).

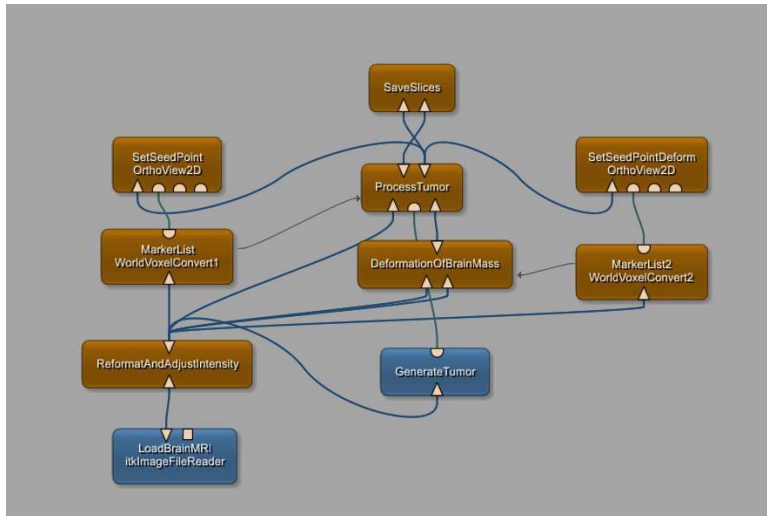


Fig. 1: Network for generating synthetic brain tumor MRI data, implemented in MeVisLab.

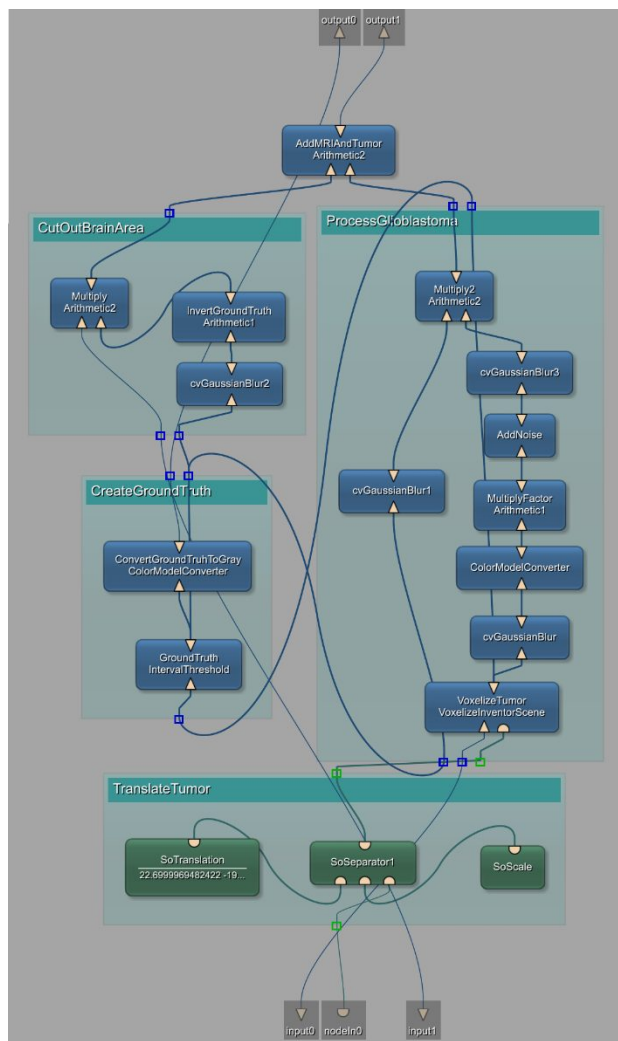


Fig. 2: The internal network of the *ProcessTumor* module.

3. RESULTS

In Figure 3, four examples of brain MRI images with real glioblastomas and a real tumor mass effect (upper row) and four brain MRI images containing synthetic glioblastomas with a simulated tumor mass effect (lower row) can be seen. The typical radiographic features of glioblastomas (thick, irregular-enhancing margins with a central necrotic core) are clearly visible in the synthetic brain MRI data. As can be seen by comparing the real MRI images in the upper row and the synthetic MRI images in the lower row, the proposed method allows to generate quite realistic looking glioblastomas, that comply with the basic radiographic features of real glioblastomas, and to simulate a simplified tumor mass effect.

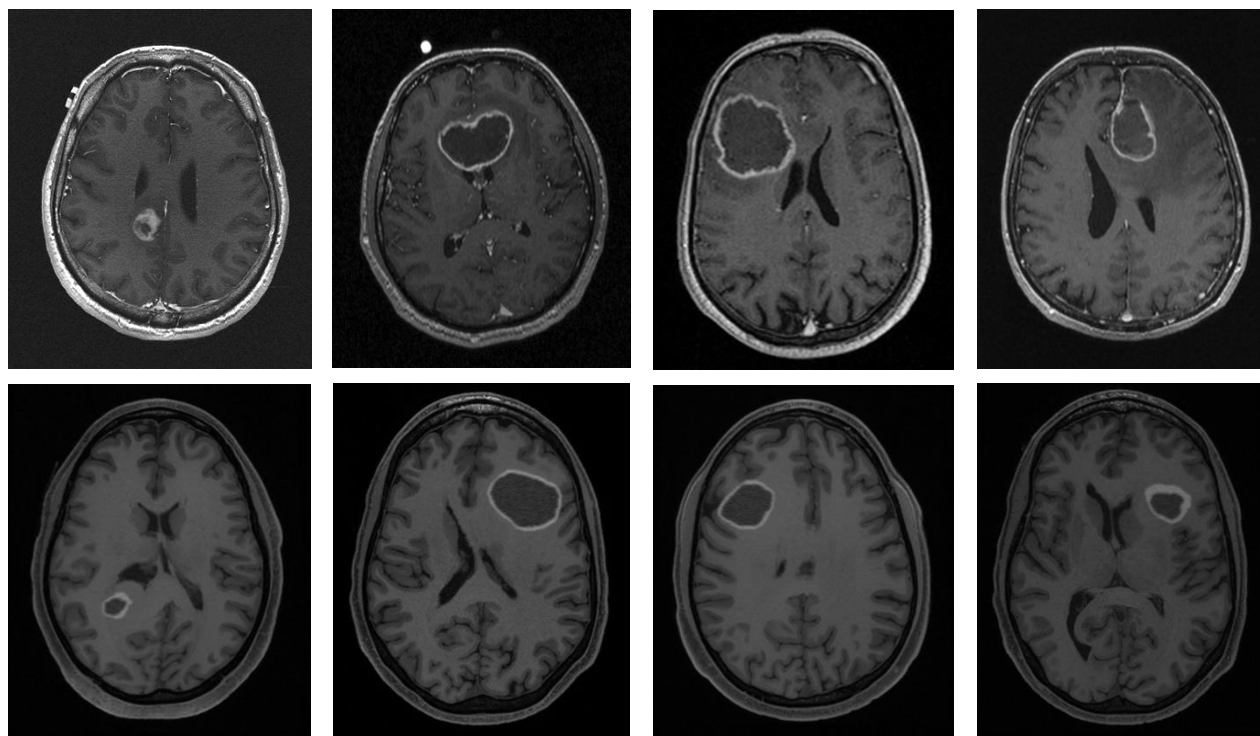


Fig. 3: Brain MRI images with real glioblastomas and a real tumor mass effect (upper row) and brain MRI images containing synthetic glioblastomas with a simulated tumor mass effect (lower row).

A brain MRI image containing a synthetic tumor (left) and the corresponding ground truth (right) can be seen in Figure 4. In Figure 5, the impact of the tumor mass effect can be seen by comparing a brain MRI image containing an artificial glioblastoma without a simulated tumor mass effect (left) and the same MRI image containing the same artificial glioblastoma with a simulated tumor mass effect (right).

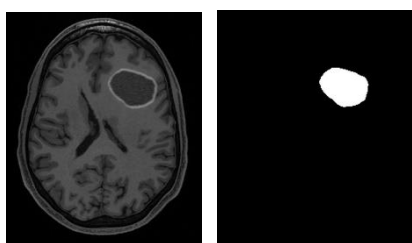


Fig. 4: Brain MRI image containing a synthetic tumor (left) and the corresponding ground truth (right).

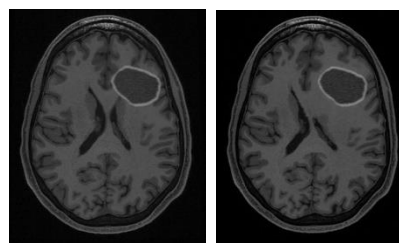


Fig. 5: Brain MRI image without tumor mass effect (left) and with tumor mass effect (right).

4. CONCLUSIONS

With the proposed method it is possible to generate realistic looking glioblastomas, insert them into brain MRI images of healthy subjects and create the corresponding ground truth in a very precise way. Furthermore, it is possible to simulate the tumor mass effect. The goal of the proposed method was to empirically generate sufficiently realistic brain MRI images and the corresponding ground truth that can subsequently be used to train a deep neural network. The accurate modeling of brain tumor growth on cell level is beyond the scope of this work. The proposed method is simple, but still has the ability to simulate all crucial characteristics of glioblastomas (appearance of the enhancing tumor and the necrotic core) in T1 weighted contrast-enhanced MRI images. In addition, an easy application via MeVisLab is presented (one click seed point selection). One advantage of inserting artificial brain tumors into MRI images of healthy subjects is that the position, shape and size of the tumor is already exactly known. Therefore, a very precise ground truth can easily be created without any required action of a human expert. Additionally, it is possible to insert several artificial tumors into the same brain MRI image, thereby maximizing the size of the resulting dataset. Since the brain MRI images of healthy subjects, that are used to insert the artificial tumors, are not contrast enhanced by the contrast agent Gadolinium, further adaptations of the proposed approach could be to simulate the effect of Gadolinium to the brain in MRI images [27]. Another adaption could be the simulation of edema or fiber bundles [28], [29]. The proposed approach may also be applied for other areas of clinical oncology and diagnostic medicine (e.g. simulation of liver tumors [30]).

ACKNOWLEDGEMENTS

The work received funding from BioTechMed-Graz in Austria (“Hardware accelerated intelligent medical imaging”), the 6th Call of the Initial Funding Program from the Research & Technology House (F&T-Haus) at the Graz University of Technology (PI: Dr. Dr. habil. Jan Egger). The corresponding source code is freely available under (November 2017):

<https://github.com/LLindn/Synthetic-Brain-Tumor-Data-Generation>

Data were provided in part by the Human Connectome Project, WU-Minn Consortium (Principal Investigators: David Van Essen and Kamil Ugurbil; 1U54MH091657) funded by the 16 NIH Institutes and Centers that support the NIH Blueprint for Neuroscience Research; and by the McDonnell Center for Systems Neuroscience at Washington University.

REFERENCES

- [1] Shen, D. et al. “Deep Learning in Medical Image Analysis,” Annual review of biomedical engineering 19, pp. 221-248 (2017).
- [2] Greiner, K. et al. “Segmentation of Aortic Aneurysms in CTA Images with the Statistic Approach of the Active Appearance Models,” Proceedings of Bildverarbeitung für die Medizin (BVM), Berlin, Germany, Springer Press, 51-55 (2008).
- [3] Lu, J. et al. “Detection and visualization of endoleaks in CT data for monitoring of thoracic and abdominal aortic aneurysm stents,” Proc. of SPIE Vol 6918, 69181F-1 (2016).
- [4] Zukic, D. et al. “Robust Detection and Segmentation for Diagnosis of Vertebral Diseases using Routine MR Images,” Computer Graphics Forum, Volume 33, Issue 6, Pages 190–204 (2014).
- [5] Zukic, D. et al. “Segmentation of Vertebral Bodies in MR Images,” Vision, Modeling, and Visualization (VMV), The Eurographics Association, pp. 135-142, (2012).
- [6] Egger, J. et al. “Interactive-cut: Real-time feedback segmentation for translational research,” Computerized Medical Imaging and Graphics 38 (4), 285-295 (2014).
- [7] Egger, J. et al. “PCG-Cut: Graph Driven Segmentation of the Prostate Central Gland,” PLOS ONE 8 (10), e76645 (2013).
- [8] Menze, B.H. et al. “The Multimodal Brain Tumor Image Segmentation Benchmark (BRATS),” IEEE Transactions on Medical Imaging 34(10), pp. 1993-2024 (2015).
- [9] Wang, J. et al. “The Effectiveness of Data Augmentation in Image Classification using Deep Learning,” Stanford, pp. 1-8 (2017).
- [10] Thurston, M. et al. “Glioblastoma,” Radiopaedia, rID: 4910 (2017).
- [11] Egger, J. et al. “GBM Volumetry using the 3D Slicer Medical Image Computing Platform,” Sci Rep., Nature Publishing Group (NPG), 3:1364 (2013).
- [12] Hogue, C. et al. “Modeling glioma growth and mass effect in 3D MR images of the brain,” MICCAI, pp. 642-50 (2007).
- [13] Prastawa, M. et al. “Synthetic Ground Truth for Validation of Brain Tumor Segmentation,” MICCAI pp. 26-33 (2005).
- [14] Egger, J. et al. “Integration of the OpenIGTlink network protocol for image guided therapy with the medical platform MeVisLab,” The international Journal of medical Robotics and Computer assisted Surgery, 8(3):282-390 (2012).
- [15] Egger, J. et al. “HTC Vive MeVisLab integration via OpenVR for medical applications,” PLoS ONE 12(3): e0173972 (2017).
- [16] Egger, J. et al. “Integration of the OpenIGTlink network protocol for image guided therapy with the medical platform MeVisLab,” The international Journal of medical Robotics and Computer assisted Surgery, 8(3):282-390 (2012).
- [17] Kuhnt, D. et al. “Fiber tractography based on diffusion tensor imaging (DTI) compared with High Angular Resolution Diffusion Imaging (HARDI) with compressed sensing (CS) – initial experience and clinical impact,” Neurosurgery, Volume 72, pp. A165-A175 (2013).
- [18] Weisstein, E. W. “Icosahedron,” <http://mathworld.wolfram.com/Icosahedron.html> (2017).

- [19] Egger, J., Mostarkic, Z., Grosskopf, S. and Freisleben, B. "A Fast Vessel Centerline Extraction Algorithm for Catheter Simulation," 20th IEEE International Symposium on Computer-Based Medical Systems, Maribor, Slovenia, pp. 177-182, IEEE Press(2007).
- [20] Egger, J. et al. "Simulation of bifurcated stent grafts to treat abdominal aortic aneurysms (AAA)," Proceedings of SPIE Medical Imaging Conference, Vol. 6509, pp. 65091N(1-6), San Diego, USA (2007).
- [21] Egger, J. et al. "Preoperative Measurement of Aneurysms and Stenosis and Stent-Simulation for Endovascular Treatment," IEEE International Symposium on Biomedical Imaging: From Nano to Macro, Washington (D.C.), USA, pp. 392-395, IEEE Press (2007).
- [22] Pfarrkirchner, B. et al. "Lower jawbone data generation for deep learning tools under MeVisLab," SPIE Medical Imaging (2018).
- [23] Lindner, L. & Egger, J. "Generation of Training Data for Brain Tumor Segmentation via MeVisLab," https://github.com/LLindn/Synthetic-Brain-Tumor_Data-Generation (2017).
- [24] Moeller, S. et al. "Multiband multislice GE-EPI at 7 tesla, with 16-fold acceleration using partial parallel imaging with application to high spatial and temporal whole-brain fMRI," *Magn Reson Med.* 63(5):1144-1153 (2010).
- [25] Milchenko, M.I. & Marcus, D. "Obscuring surface anatomy in volumetric imaging data," *Neuroinformatics.* 11(1):65-75 (2013).
- [26] Marcus, D. S. et al. "Informatics and data mining: Tools and strategies for the Human Connectome Project," *Frontiers in Neuroinformatics* 5:4 (2011).
- [27] Biswas, T. "Simulation of Contrast Enhancement of Various Brain Lesions (Without Iv Gadolinium) By Using The Neural Network," *The Internet Journal of Radiology* 14(1), pp. 1-12 (2012).
- [28] Bauer, M. et al. "A fast and robust graph-based approach for boundary estimation of fiber bundles relying on fractional anisotropy maps," 20th International Conference on Pattern Recognition (ICPR), Istanbul, Turkey, pp. 4016-4019 (2010).
- [29] Bauer, M. et al. "Boundary estimation of fiber bundles derived from diffusion tensor images," *International journal of computer assisted radiology and surgery* 6 (1), 1-11 (2011).
- [30] Hann, A. et al. "Algorithm guided outlining of 105 pancreatic cancer liver metastases in Ultrasound," *Scientific Reports* 7 (2017).